Magnetic properties of bcc Fe-Pd extended solid solutions

M. Birsan, B. Fultz, and L. Anthony*
Division of Engineering and Applied Science, mail 138-78, California Institute of Technology, Pasadena, California 91125
(Received 25 July 1996; revised manuscript received 31 January 1997)

Supersaturated Fe-Pd solid solutions were prepared by mechanical alloying. X-ray diffractometry showed that the as-milled alloys were bcc from 0–26 at. % Pd. Saturation magnetization measurements and Mössbauer spectrometry measurements were performed on these powders. Consistent interpretations of both sets of measurements were possible if the magnetic moment at the Pd atom was $0.35\mu_B$ and constant, and if the magnetic moments at Fe atoms were enhanced by neighboring Pd atoms in a way similar to the effects of Ni. [S0163-1829(97)03818-6]

I. INTRODUCTION

There has been a recent growth of research on materials prepared by mechanical alloying, driven in part by observations of nonequilibrium states of metallic alloys.[1–7] Among the many reports of phases and nonequilibrium microstructures prepared by mechanical alloying are reports of extended solid solubility in materials.[5,6,8–13] Mechanical alloying can synthesize solid solutions with broader compositional ranges than is possible by rapid quenching from high temperatures. The Hume-Rothery rules for extended solid solubility in a binary alloy predict 5 at. % solubility at high temperature when two conditions are satisfied—the difference in metallic radii of the two elements must be no greater than $\pm 15\%$, and the electronegativity must differ by no more than 0.35.[14,15] These rules are consistent with equilibrium solubility of Pd in bcc Fe: the metallic radius difference is 8%,[16] the electronegativity difference is 0.37,[16] and the maximum solubility of Pd in bcc Fe is about 3.5 at. % at 810 °C.[17] It has been shown recently that the same Hume-Rothery criteria for 5% solubility at high temperature apply to mechanical alloying at room temperature, but the solubility is 25% in a high-energy mill such as the Spex 8000.[18] The promise of such a large range of solid solubility motivated the present study of magnetic properties of bcc Fe-Pd alloys.

The magnetic properties of fcc Pd-rich Pd-Fe alloys have been studied extensively since the experimental indications of a giant magnetic moment at the Fe site, reported to be about $12.6\mu_B$.[19,20] There has been considerably less work on magnetic properties of bcc Fe-rich Fe-Pd alloys.[19–22] These previous studies were impaired by the need to work with dilute alloys, and have shown both an increase[19,22] and a decrease[21] in magnetization with Pd concentration of the bcc phase. Two of these studies on dilute alloys[19,22] showed that the magnetic moment at a Pd atom is $0.35\mu_B$, and the magnetic moments at Fe atoms with Pd neighbors are enhanced. Drittler *et al.*[23] used the Korringa-Kohn-Rostoker Green's-function method with the local-density functional approximation to obtain the magnetic moment at the Pd site and to predict that dilute substitutions of Pd in bcc Fe will cause an increase in the bulk magnetization of the alloy.

Here we report the results of a study of magnetization and hyperfine magnetic fields in Fe-Pd alloys. X-ray diffractometry showed that that the alloys were single phase bcc from 0 to 26 at. % Pd. We report that the bulk magnetization depends on Pd concentration in a way reminiscent of the Slater-Pauling curves for bcc Fe alloyed with Ni, and with fcc Fe alloyed with Pt. The hyperfine magnetic fields are consistent with a constant magnetic moment at the Pd atoms, but enhanced magnetic moments at Fe atoms that are in the neighborhood of Pd atoms.

II. EXPERIMENTAL

Alloys were prepared from elemental Fe and Pd powders of 99.95% purity by mechanical alloying in a Spex 8000 laboratory mixer/mill. Each sample of powder was sealed under an argon atmosphere in a hardened steel vial with hardened steel balls in a ratio of 1:5 by mass. Knife edges on the cap of the vial and the body of the vial were used to seal the vial with a copper gasket, and the vial was filled with argon before sealing. The milling was performed for 14 h at room temperature. Chemical concentrations of Fe, Pd, and Mn were measured in the as-milled powder by atomic emission spectrometry. The Fe concentration of the as-milled powders increased about 1.5 at. % after milling. The Mn concentration was less than 0.05 at. %. The oxygen and carbon concentrations were determined by a LECO analysis to be 0.7 and 0.4 at. %, respectively, but some of this could have been surface contamination.

X-ray-diffraction patterns of the as-milled powders were obtained at room temperature with an Inel CPS-120 diffractometer with a position-sensitive detector using monochromatized Co $K\alpha$ radiation. Mössbauer spectra were obtained in transmission geometry at room temperature with a constant-acceleration spectrometer. The radiation source was 10 mCi of ^{57}Co in a Rh matrix. Magnetization at room temperature was measured with a rotating sample magnetometer with applied magnetic fields of 240, 280, 320, 390 kA/m {3.0, 3.5, 4.0, and 4.9 kOe}. The system was calibrated by making measurements on several masses of Fe powder, and showed that the accuracy of the system was better than ± 2 emu/g. Room-temperature magnetization measurements were also obtained from some samples using a LakeShore 7300 vibrating sample magnetometer at applied fields of up to 800 kA/m. The moment meter was calibrated using a

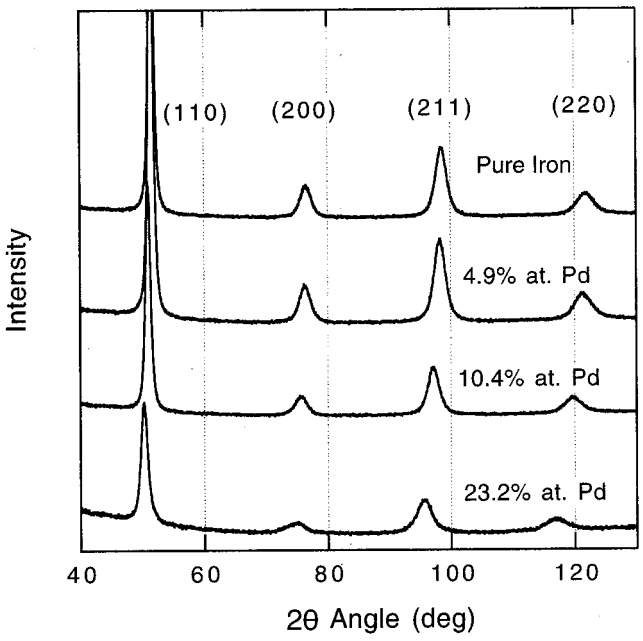

FIG. 1. X-ray-diffraction patterns of some as-milled Fe-Pd alloys.

99.995% Ni standard traceable to a NIST SRM 772 Ni standard.

III. RESULTS

X-ray diffraction patterns (Fig. 1) show that all as-milled powders with compositions 0–26 at. % Pd were bcc. The lattice parameter of the bcc unit cell was determined by the method of Nelson and Riley.[24] The lattice parameter increases monotonically with Pd concentration, as shown in Fig. 2. This near-linear dependence of lattice parameter on Pd concentration suggests that the as-milled alloys are extended solid solutions of Pd in Fe. The broadening of the x-ray-diffraction peaks is approximately the same for all as-milled materials. The average crystallite size was estimated to be 15 nm by using the method of Williamson and Hall[25] with the (110) and (220) diffractions. The root-mean-square strain was determined to be 0.9% from the same method.

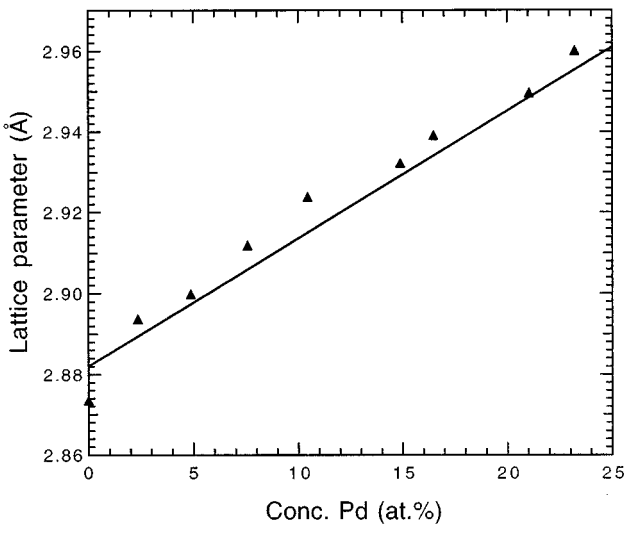

FIG. 2. X-ray lattice parameters of the as-milled Fe-Pd alloys.

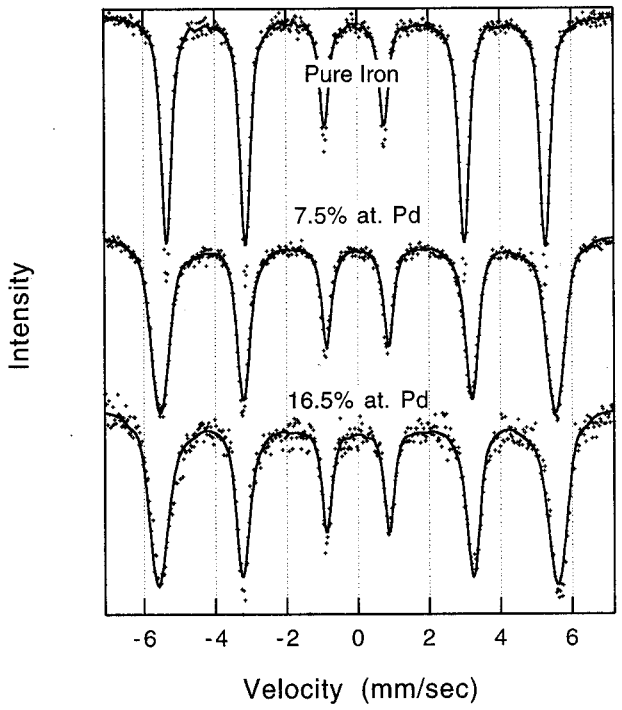

FIG. 3. Mössbauer spectra of some as-milled Fe-Pd alloys. Lines were reconstructed from the hyperfine magnetic field distributions of Fig. 4.

Mössbauer spectra of some Fe-Pd alloys and pure iron are shown in Fig. 3. Distributions of ^{57}Fe hyperfine magnetic fields (HMF) were extracted from these spectra by the method of Le Caër and Dubois,[26] and the results are presented in Fig. 4. The most prominent feature is the increase of the ^{57}Fe HMF with increasing Pd concentration. This is a

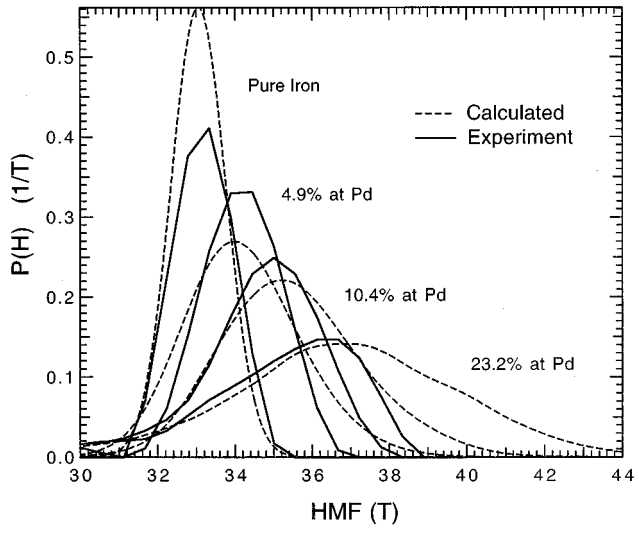

FIG. 4. Hyperfine magnetic field distributions of some Fe-Pd alloys. Solid curves: from experimental spectra. Dashed curves: from calculation described in text.

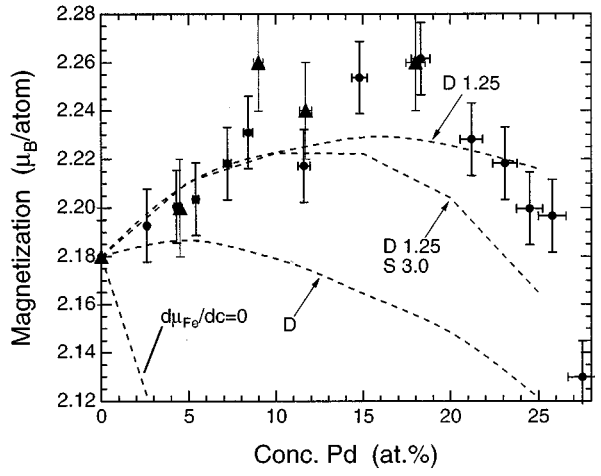

FIG. 5. Magnetization of the Fe-Pd alloys at 390 kA/m applied field at 296 K. Data were all normalized to an assumed value for pure Fe ($2.18\mu_B$/atom). Circles are experimental data from rotating sample magnetometry, triangles from vibrating sample magnetometry. Curves were calculated as described in text. The curves are not smooth because they were calculated by Monte Carlo simulations at several concentrations.

strong indication that the magnetic moment of an Fe atom is increased significantly by the neighboring Pd atoms.

The alloy magnetizations at 390 kA/m are presented in Fig. 5. Two or three samples were prepared for each Pd concentration, and several measurements were averaged for each sample. From calibration with three masses of Fe we would have errors of about $0.08\mu_B$/atom in absolute magnetizations. However, we used an equivalent mass of pure Fe as the calibration standard, whose magnetization was assumed to be $2.18\mu_B$/atom. The error bars in Fig. 5 indicate the standard deviation of the measurements. The magnetization of all alloys had saturated once the applied fields reached about 320 kA/m. Results for 800 kA/m showed a similar trend with composition, although the increase in alloy magnetization with Pd concentration was somewhat larger at 800 kA/m than at 390 kA/m. For the lowest concentrations of Pd, the addition of Pd to bcc Fe causes an increase in alloy magnetization, $dM/dc=0.7\mu_B$. This is consistent with some results from studies on dilute alloys.[19,22]

IV. DISCUSSION

For dilute alloys, the magnetization, $M(c)$, increases with Pd concentration, c. If the substitution of a Pd atom for an Fe atom serves to replace a magnetic moment of $2.18\mu_B$ with a magnetic moment of $0.35\mu_B$,[23] a positive dM/dc requires an increase in magnetic moments at Fe sites. The alloy magnetization is therefore (in units of [μ_B/atom]):

$$M(c)=0.35c+(1-c)[2.18+cd\mu_{\mathrm{Fe}}/dc], \tag{1}$$

where $d\mu_{\mathrm{Fe}}/dc$ is a positive increase in magnetic moment at Fe sites. For small c we find by comparison to the data of Fig. 5:

$$d\mu_{\mathrm{Fe}}/dc=+2.53\mu_B, \tag{2}$$

which is sufficiently large to overcome the decrease in magnetic moments at Fe sites by substitution of Pd atoms. Without an enhancement of Fe magnetic moments caused by neighboring Pd atoms, the alloy magnetization would have the composition dependence of $dM/dc=-1.83\mu_B$, indicated by the line labeled ''$d\mu_{\mathrm{Fe}}/dc=0$'' in Fig. 5. This line quickly falls well outside the error bars of our data. (This type of dependence of M on composition is typical for nonmagnetic impurities such as Al or Si in bcc Fe.)

The hyperfine magnetic field (HMF) at a particular ^{57}Fe nucleus at position $\mathbf{r}_i$, $H(\mathbf{r}_i)$, has been analyzed previously[27–30] as

$$\begin{aligned}H(\mathbf{r}_i)=H_0+(\alpha_{\mathrm{CP}}+\alpha_{\mathrm{CEP}}f(0))(\mu_{\mathrm{Fe}}(\mathbf{r}_i)-\mu^0_{\mathrm{Fe}})\\ +\alpha_{\mathrm{CEP}}\sum_{\mathbf{r}_j} f(\mathbf{r}_j)[(\delta(\mathbf{r}_j)\mu_{\mathrm{Pd}}(\mathbf{r}_j)\\ +[1-\delta(\mathbf{r}_j)]\mu_{\mathrm{Fe}}(\mathbf{r}_j))-\mu^0_{\mathrm{Fe}}],\end{aligned} \tag{3}$$

where the HMF of ^{57}Fe in pure bcc Fe H_0 is -33.0 T at 296 K. The Kroneker delta, $\delta(\mathbf{r}_j)$, equals 1 if the site $\mathbf{r}_j$ is occupied by a Pd atom, and zero if it is occupied by an Fe atom. The magnetic moments of Pd and Fe atoms are denoted as μ_{Pd}, and μ_{Fe}, respectively. The second and third terms of Eq. (3) are the local and nonlocal contributions to the ^{57}Fe HMF. The second term of Eq. (3) is the perturbation of the ^{57}Fe HMF caused by the change in magnetic moment at the ^{57}Fe atom itself. The magnetic moment at an Fe atom depends on the number of Pd atoms in its nearest-neighbor shells:

$$\mu_{\mathrm{Fe}}(\mathbf{r}_i)=\mu^0_{\mathrm{Fe}}+\sum_{\mathbf{r}_j}\delta(\mathbf{r}_j)g^{\mathrm{Fe}}_{\mathrm{Pd}}(|\mathbf{r}_j-\mathbf{r}_i|), \tag{4}$$

where each parameter $g^{\mathrm{Fe}}_{\mathrm{Pd}}(r_j)$ is the perturbation of the magnetic moment at an Fe atom caused by a Pd atom in its jth nearest-neighbor shell, and μ^0_{Fe} is the magnetic moment of an Fe atom in pure bcc Fe. The factor in square brackets in Eq. (3) is the difference between the magnetic moment at a site in the alloy and a site in pure bcc Fe. This change in magnetic moment affects $H(\mathbf{r}_i)$ through the conduction-electron polarization response parameters: $\alpha_{\mathrm{CEP}}\{f(\mathbf{r}_j)\}=\{-1.15,-0.35,+0.25\}[T/\mu_B]$, as determined by calibration experiments with nonmagnetic solutes.[28,30] The set of conduction-electron response parameters, $\alpha_{\mathrm{CEP}}\{f(\mathbf{r}_j)\}$, could be different for large Pd atoms than for solutes such as Ni and Co. The conduction-electron polarization scales with the magnetic moment located at the site, however. Owing to the small magnetic moment at the Pd atom, the calculation of the HMF is insensitive to the choice of these parameters. The set of conduction-electron polarization parameters, $\alpha_{\mathrm{CEP}}\{f(\mathbf{r}_j)\}$, could also be altered for Fe atoms having Pd neighbors, but here we assume that Fe atoms with Pd neighbors polarize the conduction electrons with the same proportionality to site moment as do Fe atoms in pure Fe metal.

The second set of parameters required to calculate the ^{57}Fe HMF are the magnetic moments and their changes with local chemical environment. We use magnetic moments of 2.18 and $0.35\mu_B$ for Fe and Pd atoms, respectively.[19,21,22] With increasing numbers of Pd neighbors, we assume that the magnetic moment at the Pd atom remains unchanged.

This is expected for the same reason as for Ni and Co atoms,[28,29] whose $d\uparrow$ states are full, having energies below the Fermi level. Any increase in the magnetic moment at either a Pd, Ni, or Co atom therefore must occur by a decrease in $d\downarrow$ occupancy at the atom, causing an energetically costly loss of charge at the atom. On the other hand, since there are empty $3d\uparrow$ states at Fe atoms, a Pd atom at $\mathbf{r}_j$ can shift the balance of both the $3d\uparrow$ and $3d\downarrow$ electrons of the Fe atom, leading to a perturbation in the magnetic moment at the Fe atom as in Eq. (4). The set of magnetic moment perturbations of Fe atoms at the jth neighbor position of a Pd atom, $\{g_{\mathrm{Pd}}^{\mathrm{Fe}}(j)\}$, has been calculated by Drittler *et al.* as $\{0.109,0.021,0.034,0.021,0.011\}[\mu_B]$. There is a constraint on these parameters, however, required for consistency with Eq. (2):[28]

$$d\mu_{\mathrm{Fe}}/dc=\sum_{\mathbf{r}_j} N_j g_{\mathrm{Pd}}^{\mathrm{Fe}}(j), \tag{5}$$

where N_j is the number of sites in the jth nearest-neighbor shell. Using $\{N_j\}=\{8,6,12,24,8\}$[sites], the parameters of Drittler *et al.* provide $d\mu_{\mathrm{Fe}}/dc=2.00\mu_B$. We have performed our calculations of the ^{57}Fe HMF with both the original parameters of Drittler *et al.*, and with the parameters multiplied by the factor of 1.25 required to ensure consistency with Eq. (2).

Equations (1) and (4) were used to calculate the alloy magnetization, $M(c)$, and the distribution of hyperfine magnetic fields (HMF). It is not possible to calculate the HMF distribution analytically with Eqs. (3) and (4) since multiple centers are involved for the terms in $H(\mathbf{r}_i)$. We therefore calculated HMF distributions and alloy magnetizations simultaneously with a Monte Carlo code described previously.[30] The Monte Carlo calculation first generates around an ^{57}Fe atom a configuration of atoms that is characteristic of a bcc solid solution. The code next evaluates the magnetic moment at each site [$0.35\mu_B$ for Pd, and Fe moments obtained with Eq. (4)]. The average moment of this atom configuration is stored, as is the HMF at the central ^{57}Fe atom calculated with Eq. (3). A configuration of atoms is generated, and a histogram of HMF's was obtained after about 1000 configurations.

The curve labeled ''*D*'' in Fig. 5 was obtained from $M(c)$ of Eq. (1) when the $\{g_{\mathrm{Pd}}^{\mathrm{Fe}}(j)\}$ parameters of Drittler *et al.*[23] were used directly in Eq. (4). The magnetization so calculated is too small at most Pd concentrations. We attribute this to the $\{g_{\mathrm{Pd}}^{\mathrm{Fe}}(j)\}$ parameters of Drittler *et al.* being a bit too small. The curve labeled ''*D* 1.25'' was obtained with the set of parameters $\{g_{\mathrm{Pd}}^{\mathrm{Fe}}(j)\}$ provided by Drittler *et al.*[23] after being multiplied by a factor of 1.25 to ensure consistency with Eq. (2). Agreement with the experimental data is much improved, although the magnetization may still be a bit small at around 15 at. % Pd. Although this discrepancy is barely above our experimental errors, it would be consistent with the Pd moment increasing to $0.55\mu_B$ from its value of $0.35\mu_B$ in Fe-rich alloys. We believe a more reliable trend is the decrease in magnetization observed for Pd concentrations above 18 at. %. This trend shows that the magnetization at high Pd concentrations is probably affected by the saturation of the Fe magnetic moment. As an Fe atom has increasingly more Pd neighbors, the magnetic moment of the Fe atom does not increase steadily, but reaches a saturation value. To implement saturation in the calculation, we allowed the Fe magnetic moment to initially increase with Pd concentration as provided by the set of parameters $\{g_{\mathrm{Pd}}^{\mathrm{Fe}}(j)\}$. At 2/3 of the saturation moment, however, the effects of additional Pd neighbors were halved. Finally, no Fe atoms were allowed to have magnetic moments larger than the saturation moment, which was an adjustable parameter. We found that the best fit to the decrease in magnetization for Pd concentrations greater than 18 at. % was obtained when the Fe moment saturated at $3.0\mu_B$. This calculated magnetization curve is shown as a solid line in Fig. 5 with the label ''*D* 1.25 *S* 3.0.'' This particular calculation used the $\{g_{\mathrm{Pd}}^{\mathrm{Fe}}(j)\}$ parameters of Ref. 23 multiplied by 1.25, a saturation of the Fe magnetic moment at $3.0\mu_B$, $\mu_{\mathrm{Pd}}=0.35\mu_B$, and $\mu_{\mathrm{Fe}}^0=2.18\mu_B$.

We calculated the ^{57}Fe HMF distribution with the same parameters used to calculate the alloy magnetization. The histogram of HMF data was convolved with a Gaussian function (shown in Fig. 4 for 0% Pd) to allow for comparison to the experimental line shapes. The HMF distributions shown in Fig. 4 were obtained for the same parameters that gave the best fit to the alloy magnetization data (i.e., the $\{g_{\mathrm{Pd}}^{\mathrm{Fe}}(j)\}$ parameters of Drittler *et al.*[23] multiplied by 1.25, a saturation of the Fe magnetic moment at $3.0\mu_B$, $\mu_{\mathrm{Pd}}=0.35\mu_B$, and $\mu_{\mathrm{Fe}}^0=2.18\mu_B$). The agreement between calculated and experimental curves in Fig. 4 is good over the full range of Pd concentrations. Without saturation of the Fe moment, at high Pd concentrations the high-field tail on the calculated HMF distribution, which is absent in the experimental distribution, was even stronger than shown in Fig. 4. Incidentally, if the Pd atoms did not enhance the magnetic moments of neighboring Fe atoms (i.e., $\{g_{\mathrm{Pd}}^{\mathrm{Fe}}(j)\}=0$), the mean HMF would decrease to 29.2 T with a Pd concentration of 25%.

The model of ^{57}Fe hyperfine magnetic fields upon which Eq. (3) is based is known to work well for nonmagnetic solutes that do not perturb strongly the magnetic moments of neighboring Fe atoms. For solutes that cause stronger magnetic disturbances, the model was shown successful for bcc Fe-Ni (Ref. 28) and bcc Fe-Co (Ref. 29) alloys. The success of the HMF calculations shown in Fig. 4 should be considered as much a test of the HMF model as a test of the magnetic parameters of bcc Fe-Pd. It is satisfying that the same set of magnetic parameters accounts for both the alloy magnetizations and the hyperfine magnetic field distributions of bcc Fe-Pd alloys. These parameters are $\{g_{\mathrm{Pd}}^{\mathrm{Fe}}(j)\}=\{0.136,0.026,0.042,0.026,0.014\}[\mu_B]$, a saturation of the Fe magnetic moment at $3.0\mu_B$, $\mu_{\mathrm{Pd}}=0.35\mu_B$, and $\mu_{\mathrm{Fe}}^0=2.18\mu_B$.

V. CONCLUSION

We used high-energy ball milling to synthesize bcc Fe-Pd alloys with greatly extended Pd solubilities. The alloys were shown by x-ray diffractometry to be entirely bcc phase to compositions of 26 at. % Pd. We measured the saturation magnetization, M, and the Mössbauer spectra of these powders. The data of magnetization versus Pd concentration are much like the Slater-Pauling curve for bcc Fe-Ni alloys. We

found that $dM/dc = 0.7\mu_B$ for low Pd concentrations, c. Assuming a constant magnetic moment at the Pd site of $0.35\mu_B$, we found that Pd atoms cause a net increase in the magnetic moments at Fe sites of $d\mu_{\mathrm{Fe}}/dc = 2.53\mu_B$. At higher Pd concentrations the magnetic moment at the Fe sites saturates to a maximum value of about $3.0\mu_B$. The magnetic behavior of Fe-Pd alloys is much like Fe-Ni and Fe-Pt alloys, perhaps since Ni, Pd, and Pt all lie in the same column of the periodic table. Mössbauer hyperfine magnetic-field distributions were calculated by explicit consideration of the core and conduction electron responses to the magnetic moments in the alloys. With no adjustable parameters, these calculations provided a reasonable agreement with the measured HMF distributions of bcc Fe-Pd alloys.

ACKNOWLEDGMENTS

One of the authors, M. Birsan, thanks the Canadian NSERC program for support. This work was supported by the National Science Foundation under Grant No. DMR-9213447.

*Present address: Department of Physics and Astronomy, University of Toledo, McMaster Hall 2017, 2801 W. Bancroft Street, Toledo, OH 43606-3390.

[1] C. C. Koch, O. B. Cavin, C. G. McKamey, and J. O. Scarbrough, Appl. Phys. Lett. **43**, 1017 (1983).
[2] R. B. Schwarz, R. R. Petrich, and C. K. Saw, J. Non-Cryst. Solids **76**, 281 (1985).
[3] E. Hellstern, H. J. Fecht, Z. Fu, and W. L. Johnson, J. Mater. Res. **4**, 1292 (1989).
[4] H. J. Fecht, E. Hellstern, Z. Fu, and W. L. Johnson, Adv. Powder Metall. **1–2**, 111 (1989).
[5] B. Fultz, G. LeCaër, and P. Matteazzi, J. Mater. Res. **4**, 1450 (1989).
[6] E. Hellstern, H. J. Fecht, Z. Fu, and W. L. Johnson, J. Appl. Phys. **65**, 305 (1989).
[7] J. S. C. Jang and C. C. Koch, J. Mater. Res. **5**, 325 (1990).
[8] E. Hellstern, L. Schultz, R. Bormann, and D. Lee, Appl. Phys. Lett. **53**, 1399 (1988).
[9] C. C. Koch, Ann. Rev. Mater. Sci. **19**, 121 (1989).
[10] A. Calka and A. P. Radlinski, Scr. Metall. **23**, 1497 (1989).
[11] K. Uenishi, K. F. Kobayashi, K. N. Ishihara, and P. H. Shingu, Mater. Sci. Eng. A **134**, 1342 (1991).
[12] M. V. Zdujic, K. F. Kobayashi, and P. H. Shingu, J. Mater. Sci. **26**, 5502 (1991).
[13] D. K. Mukhopadhyay, C. Suryanarayana, and F. H. Froes, Scr. Metall. Mater. **30**, 133 (1994).
[14] W. Hume-Rothery and G. V. Raynor, *The Structure of Metals and Alloys* (Institute of Metals, London, 1962).
[15] L. S. Darken and R. W. Gurry, *Physical Chemistry of Metals* (McGraw-Hill, New York, 1953), p. 74.
[16] E. T. Teatum, K. A. Gschneidner, Jr., and J. T. Waber, Compilation of Calculated Data Useful in Predicting Metallurgical Behavior of the Elements in Binary Alloy Systems, Los Alamos Laboratory Report No. 4003 (1968).
[17] T. B. Massalski, *Binary Alloy Phase Diagrams* (ASM, Metals Park, OH, 1986).
[18] C. Bansal, Z. Q. Gao, L. B. Hong, and B. Fultz, J. Appl. Phys. **76**, 5961 (1994).
[19] A. M. Clogston, B. T. Matthias, M. Peter, H. J. Williams, E. Corenzwit, and R. J. Sherwood, Phys. Rev. **125**, 541 (1962).
[20] G. J. Nieuwenhuys, Adv. Phys. **24**, 515 (1975).
[21] M. Fallot, Ann. Phys. (Paris) **10**, 291 (1938).
[22] M. F. Collins and G. G. Low, Proc. Phys. Soc. London **86**, 535 (1965).
[23] B. Drittler, N. Stefanou, S. Blugel, R. Zeller, and P. H. Dederichs, Phys. Rev. B **40**, 8203 (1989).
[24] J. B. Nelson and D. P. Riley, Proc. Phys. Soc. London **57**, 126 (1945).
[25] H. P. Klug and L. E. Alexander, *X-Ray Diffraction Procedures* (Wiley-Interscience, New York, 1974), pp. 652–665.
[26] G. Le Caër and J. M. Dubois, J. Phys. E **12**, 1083 (1979).
[27] I. Vincze and I. A. Campbell, J. Phys. F **3**, 647 (1973).
[28] B. Fultz and J. W. Morris, Jr., Phys. Rev. B **34**, 4480 (1986).
[29] H. H. Hamdeh, B. Fultz, and D. H. Pearson, Phys. Rev. B **39**, 11 233 (1989).
[30] B. Fultz, in *Mössbauer Spectroscopy Applied to Magnetism and Materials Science*, edited by G. J. Long and F. Grandjean (Plenum, New York, 1993), Vol. 1, p. 1.